Journal of Hazardous Materials, Volume 511, June 2026, Article number 142281
DOI: 10.1016/j.jhazmat.2026.142281

Carbon metabolic homogenization is linked to microbial competition and antimicrobial resistance in soils under forest-to-cropland conversion

Shaoyang Zhang[1,2#], Tianlun Zhang[1,2#], Shuai Du[1,3*], Zhugen Yang[4], Shengen Liu[5*], Guiyao Zhou[6,7], Manuel Delgado-Baquerizo[6], Dong Zhu[1,2,3*]

[1] State Key Laboratory of Regional and Urban Ecology, Ningbo Observation and Research Station, Institute of Urban Environment, Chinese Academy of Sciences, Xiamen 361021, China;
[2] University of Chinese Academy of Sciences, Beijing 100049, China;
[3] Zhejiang Key Laboratory of Pollution Control for Port-Petrochemical Industry, CAS Haixi Industrial Technology Innovation Center, Ningbo 315830, China;
[4] School of Water, Energy and Environment, Cranfield University, Cranfield, Bedfordshire MK43 0AL, United Kingdom;
[5] College of Forestry, Fujian Agriculture and Forestry University, Fuzhou 350000, China;
[6] Laboratorio de Biodiversidad y Funcionamiento Ecosistémico, Instituto de Recursos Naturales y Agrobiología de Sevilla (IRNAS), CSIC, Sevilla 41012, Spain;
[7] German Centre for Integrative Biodiversity Research (iDiv), Leipzig 04103, Germany;

[*] Correspondence should be addressed to: dzhu@iue.ac.cn (Dong Zhu); sdu@iue.ac.cn (Shuai Du); liu_iae@163.com (Shengen Liu)
[#] These authors contribute equally.

Published by Elsevier. This is the Author Accepted Manuscript issued with: Creative Commons Attribution License (CC:BY 4.0).
The final published version (version of record) is available online at DOI:10.1016/j.jhazmat.2026.142281. Please refer to any applicable publisher terms of use.

Abstract

Global agricultural expansion by converting natural forests into croplands often leads to soil functional homogenization and antimicrobial resistance enhancement, threatening ecosystem services. However, the associations between microbial carbon metabolic homogenization and antimicrobial resistance remain largely unknown. Here, we collected 240 paired forest and cropland soil samples from the most intensively farmed Yangtze River Basin in China, and constructed a novel framework based on microbial functional traits to decipher the role of carbon metabolic homogenization on antimicrobial resistance via microbial competition for metabolites. Using genome-scale metabolic models, we found that carbon metabolic homogenization was associated with a shift in microbial interactions from cooperation toward competition, with a 45.6% increase in competitive interactions that coincided with a 35.6% higher antimicrobial resistance gene (ARG) diversity. This shift was accompanied by smaller genome sizes and higher 16S rRNA copy numbers, indicating fast-growing, resource-acquisitive microbial strategies. Metabolic transfer analyses further revealed less cooperation relationships among microbial communities in cropland soils than in forest soils, indicating an intensified battle for communal metabolites and an attenuated exchange for complementary metabolites. Together, these findings provide a new framework to understand the association between carbon metabolic homogenization and soil antimicrobial resistance risks from the perspective of microbial traits and interactions under land use change.

Keywords: Soil functional homogenization; Microbial carbon metabolism; Antimicrobial resistance genes; Microbial competition; Land-use change

1. Introduction

Functional homogenization refers to the increasing similarity of functional attributes among communities under environmental change [1]. In soil ecosystems, this process may reduce ecosystem buffering capacity, constrain functional diversity, and weaken ecosystem multifunctionality, thereby increasing ecosystem vulnerability [2,3]. Such functional shifts are particularly relevant under ongoing agricultural intensification, which is increasingly reshaping land use patterns worldwide. Global food demand is projected to increase by approximately 70% by the year 2050 relative to 2005–2007 levels [4], and has intensified the utilization of land resources, making the sustainable management of agroecosystems a central challenge for ensuring food production and security [5].

Agricultural soil is a major reservoir of microbial resources and a hotspot for antimicrobial resistance genes (ARGs), which can be attributed to fertilizer driven organic matter inputs and pesticide driven antibiotic selective pressures. In addition to these direct agricultural inputs, differences in human activity intensity may also shape ARG patterns by affecting the extent of land disturbance, and the environmental dissemination of resistance determinants [6,7]. Land management can modify soil environmental conditions through changes in nutrient inputs, vegetation cover, and microbial functions [8]. Land-use change from forests to croplands is the most widespread form of agricultural intensification [9], particularly in large river basins sustaining rich soil biodiversity and ecosystem functions [10,11]. Cropland in the Colombian Orinoco savannas has expanded by 490 thousand hectares from the year 2007–2018 [12], while cropland expansion has resulted in the loss of approximately 54.2 million hectares of forests in the Amazon Basin from the year 2001–2020 [13]. The conversion of natural ecosystem to cropland has been reported to aggravate microbial homogenization [14], or ARG dissemination [15], posing risks to human health [16]. However, the relationship between functional homogenization and ARG diversity under forest-to-cropland conversion remains poorly understood.

Carbon metabolic homogenization is an important form of functional homogenization, indicating that microbes tend to utilize similar carbon source, thereby forming a simplified

metabolic profile in a microbial community [2]. The homogenization is largely mediated by carbohydrate-active enzymes (CAZymes) which regulate the breakdown, synthesis, and modification of carbon compounds and are central to carbon cycling [17]. Land-use change from forests to croplands can simplify vegetation structure and reduce organic matter inputs by disrupting the balance between litter decomposition and carbon mineralization [18]. This change may narrow carbon source diversity and limit microbial carbon metabolic capacity [19], forcing microbes to compete for similar carbon source by shifting their functional traits to survive intensified competition. Although land conversion to agriculture is known to induce taxonomic homogenization [20,14], the ecological mechanisms and consequences of carbon metabolic homogenization remain to be clarified.

Land-use intensification has accelerated the spread of ARGs, raising urgent ecological and public health concerns [21]. Microbes carrying ARGs can not only survive antimicrobial exposure, but also obtain strong competitive advantage to suppress their rivals by releasing antibiotics [22]. In parallel, carbon source simplification in soils can result in intensified microbial competition [2]. However, the potential association between microbial carbon metabolism, competition, and ARG diversity has not been clearly established. Recently, the genome-scale metabolic models (GSMMs) have provided a powerful framework for investigating the interactions with microbial communities, and has revealed key ecological mechanisms of microbial metabolic preference and the tradeoff between competition and cooperation [23,24]. Previous studies have advanced our understanding of the microbial metabolic cooperation within the community for acquiring complementary resources, thereby reducing the overlapped niche of resource utilization [25] and mitigating environmental pressures [26]. These studies highlight the strong potential of GSMMs for predicting microbial interactions and metabolic mechanisms. However, how microbial metabolic competition for carbon sources can influence ARG diversity, especially in the context of intensified agriculture, remains largely unclear.

Here, we investigated how forest to cropland conversion is associated with carbon metabolic homogenization and its relationship with ARG diversity across the Yangtze River Basin, a region spanning over 1.8 million km^2 and supporting more than 25 million people [27].

As one of China's most intensively farmed regions, it contains over a third of arable land, and faces mounting pressure from land-use intensification. The land-use change is likely to reduce the diversity of carbon sources and homogenize microbial carbon metabolic functions [19]. This change may intensify microbial competition and increase the spread of ARGs, as microbial resistance traits may have a survival advantage under resource constraints. To address this hypothesis, we collected 240 soil samples from paired forests and croplands across the basin (Fig. 1A), used microbial life history traits to characterize ecological strategies, and applied GSMMs to evaluate microbial cooperation and competition. We further assessed how carbon metabolic homogenization may influence ARG diversity by altering microbial interactions. Our study highlights the ecological consequence of functional homogenization and provides novel insights for developing sustainable policies and management strategies in croplands across large river basins.

2. Methods

2.1 Study sites and sample collection

The Yangtze River, the world's third-longest and China's largest river, originates from the Qinghai-Xizang Plateau and flows eastward into the East China Sea [28]. In 2020, we established a 3000 km sampling transect along the main stream of the Yangtze River from the upper to the lower reaches (103°66′ E-119°68′ E, 28°25′ N-32°23′ N, 7–553 m a.s.l.), spanning eight provinces: Yunnan, Sichuan, Chongqing, Hubei, Jiangxi, Anhui, and Jiangsu (Fig. 1).

The Yangtze River Basin encompasses a wide range of climatic zones, transitioning from alpine conditions on the Qinghai-Xizang Plateau to subtropical monsoon climates in the east. Annual precipitation averages 1,100 mm and generally increases from northwest to southeast, reflecting strong geographic and topographic heterogeneity [29]. Most of the basin experiences a humid subtropical monsoon climate, with hot, rainy summers and mild, wet winters. Mean annual temperature (MAT) ranges from –4 °C in the western highlands to 16–18 °C in the middle and lower reaches [30]. Site-specific MAT and mean annual precipitation (MAP) were obtained from WorldClim 2.1 (https://www.worldclim.org). Vegetation types vary markedly across the basin, ranging from cold-temperate montane coniferous forests in the west to

subtropical evergreen broadleaf forests in the east. Vegetation surveys were conducted using standardized protocols [31], recording dominant vegetation types, species richness (trees, shrubs, herbs), and litter dry weight. Key forest species included *Cinnamomum camphora*, *Platycladus orientalis*, and *Populus tomentosa*, with regionally abundant species such as *Phoebe zhennan*, *Quercus variabilis*, and *Cryptomeria fortunei*. In the upper and middle reaches, particularly around Chengdu and Chongqing, cropland intensification and livestock operations contribute substantial nutrient and microbial inputs via wastewater discharge [32]. To account for socioeconomic drivers, we compiled eight variables from the China Statistical Yearbook, China City Statistical Yearbook, and China Population Census Yearbook. These included forestry-related indicators (forestry GDP, forestry GDP per capita) and cropland-related indicators (total population, GDP per capita, agricultural GDP per capita, grain yield per unit area, fertilizer application, and pesticide use).

We collected soil samples from 20 sampling locations distributed along the main stream of the Yangtze River Basin from the upper to the lower reaches. At each location, sampling was conducted on both the northern and southern banks of the river to reduce potential bias caused by bank-related heterogeneity. On each bank, paired forest and cropland sites were established within each location, and three replicate plots were sampled for each land use type. This sampling design therefore generated 12 samples per location (2 banks × 2 land use types × 3 replicates), resulting in 240 samples in total across the 20 locations, including 120 forest samples and 120 cropland samples (Fig. 1A). Within each bank, forest and cropland sites were located approximately 2 km apart to ensure comparable climatic and soil conditions while differing in land use type. Cropland sites were limited to wheat fields and orchards to reduce variability. At each site, we established a 10 m × 10 m plot and randomly collected five soil cores (0–10 cm depth, 2 cm diameter), which were then mixed and sieved through a 2 mm mesh to form one composite sample. Each composite sample was divided into two portions: one was used for soil physicochemical and enzyme activity assessments, and the other was stored at –80°C for DNA extraction.

2.2 Soil properties measurement

Soil pH, organic carbon (SOC), total nitrogen (TN), total phosphorus (TP), moisture, and

157 NH_4^+-N concentrations were measured using methods consistent with our previous study [31].
158 Soil pH was measured using a Sartorius PB-10 pH meter (Germany) in a 1:2.5 soil-water slurry.
159 SOC was determined via the potassium dichromate oxidation method, while TN and TP were
160 measured using the Kjeldahl and Olsen methods, respectively. Soil moisture was assessed by
161 oven-drying samples at 105 °C to a constant mass. NH_4^+-N was extracted with 2 M KCl and
162 analyzed using a Smartchem200 discrete automatic analyzer (Alliance, France). Five soil
163 functions related to nutrient cycling were quantified: soil carbon mineralization, and the
164 potential activities of β-1,4-glucosidase (S-β-GC), β-1,4-N-acetyl-glucosaminidase (S-NAG),
165 leucine aminopeptidase (S-LAP), and acid phosphatase (S-ACP). Soil carbon mineralization
166 rates were determined via the aerobic incubation method [33]. The potential activities of the
167 enzymes were measured using a soil enzyme assay kit (Beijing Solarbio Science & Technology
168 Co., Ltd.). Soil enzyme activity was calculated using the average approach, which involved z-
169 score transformation of each soil function followed by averaging the standardized values [34].

170 **2.3 Microbial metagenomic sequencing, assembly, and binning**

171 Soil DNA was extracted using the FastDNA Spin Kit (MP Biomedicals, Cleveland, USA)
172 according to the manufacturer's protocol. DNA quality was assessed via 1% agarose gel
173 electrophoresis, and concentration was measured using a NanoDrop 1000 spectrophotometer.
174 High-throughput sequencing was performed on an Illumina HiSeq 2000 platform by Majorbio
175 Biotechnology Co., Ltd. (Shanghai, China). Low-quality reads (Q score ≤ 20, length < 50, or
176 containing N bases) were filtered using the fastp software. All sequence data have been
177 deposited in the National Center for Biotechnology Information (NCBI) under BioProject
178 accession number PRJNA1462470. Contigs with a minimum length of 1000 bp (or 1500 bp for
179 metaBAT2) were assembled and used for genome binning with metaWRAP (v1.3.2),
180 incorporating metaBAT2 (v2.12.1), MaxBin2 (v2.2.6), and CONCOCT (v1.0.0) [35]. Bins were
181 refined using the metaWRAP bin_refinement module with parameters -c 90 -x 5, retaining only
182 MAGs with > 90% completeness and < 5% contamination for subsequent analysis [36].

183 Refined genome bins were dereplicated using dRep (v3.5.0) with parameters -pa 0.9 and -
184 sa 0.95 [37]. We selected a secondary ANI threshold of 0.95 because it represented an
185 intermediate level of dereplication stringency in our dataset, retaining 114 MAGs compared

with 152 and 109 MAGs at thresholds of 0.99 and 0.90, respectively. Genome size was estimated by dividing the total genome size by the sum of completeness and contamination [38]. Taxonomic classification of MAGs was performed using the GTDB-Tk classify_wf workflow against the GTDB genome database (Release 202). MAGs were quantified with CoverM (v0.7.0) in genome mode, using paired reads and the parameter --method relative_abundance. The resulting MAG table included relative abundance data and unmapped read percentages for each sample. A phylogenetic tree for bacterial and archaeal MAGs was constructed using multiple sequence alignments generated by GTDB-Tk and visualized using iTOL (v6.6). ARGs were analyzed with the local ARG-OAP tool (version 3.2) using the structured SARG database, applying the following thresholds: E-value $\leq 10^{-7}$, identity $\geq 80\%$, and hit length $\geq 75\%$ [39]. To compare relative ARG abundances across samples, ARG counts were normalized to total cell abundance and expressed as copies per cell. High-risk ARGs were defined as those in the top 25% based on the human health risk index (RI) from previous studies [40].

2.4 Microbial community life history trait calculation

Reads were mapped to the functional databases KEGG, eggNOG, and CAZy [41], with data aggregated at the following levels: (1) pathways from KEGG, (2) functional categories from eggNOG, and (3) gene families from CAZy include glycoside hydrolases (GH), auxiliary activities (AA), polysaccharide lyases (PL), carbohydrate esterases (CE), glycosyl transferases (GT), and carbohydrate-binding modules (CBM) [42]. These databases provided complementary classifications of functional genes. The average 16S rRNA gene copy number was calculated as the ratio between the coverage of 16S rRNA genes and the estimated genome count, while the average genome size was obtained by dividing the total assembled base pairs by the genome count [43]. Bacterial life history strategies were classified according to Piton et al. (2023), using community-aggregated trait (CAT) databases encompassing life history traits, eggNOG orthologous categories, CAZyme families, and KEGG pathways. Multivariate constrained ordination analysis (MCOA) was applied to integrate data from these four databases and identify principal axes explaining variation in soil microbial community traits. Prior to analysis, all microbial CATs were log-transformed ($\log X + 1$) to improve normality and standardized to have a mean of zero and variance of one [45]. The R (version 4.2.3) package

ade4 was used for MCOA analysis. Coordinates from the first and second MCOA dimensions were extracted as latent variables, representing the positions of microbial communities within the global trait space.

2.5 Construction of co-occurrence and genome-scale metabolic networks

Co-occurrence networks were constructed using the *Hmisc* and *igraph* packages in R with the Spearman correlation method. The random matrix theory (RMT) was applied to determine the threshold for strong correlations, using the MAG table tool on the iNAP website [46]. Pairs of genera with correlations above the RMT threshold (Spearman's $|\rho| \geq$ threshold) and significant associations (Benjamini-Hochberg adjusted $p < 0.05$) were considered statistically robust [26]. The networks were visualized in Gephi (version 0.10.1) using the Fruchterman–Reingold layout.

GSMMs for all MAGs were constructed using CarveMe (v1.4.1) with default parameters. Coding sequences for each MAG were predicted using Prokka [47]. Pairwise interactions between GSMMs were predicted using PhyloMint [48], which provided the metabolic complementarity index ($MI_{Complementarity}$) to assess cooperation and the competition index ($MI_{Competition}$) to gauge competition. $MI_{Complementarity}$ and $MI_{Competition}$ values were calculated using the RMT cutoff tool on the iNAP website. Interactions exceeding the RMT threshold were used to construct complementarity and competition networks, where edges represent interactions. Unidirectional interactions surpassing the threshold were classified as commensalism (RMT: 0.229)/amensalism (RMT: 0.672), while bidirectional interactions were classified as mutualism/competition [26]. MAGs were classified into either the forest group or the cropland group according to their relative abundance patterns [26]. Specifically, a MAG was assigned to a given group if its relative abundance was higher in that group than in the other and this pattern was observed in more than 40% of the samples. MAGs that did not meet this criterion were considered to be shared between both groups. These two categories were evaluated independently and were therefore not mutually exclusive. In total, 71 MAGs were assigned to the forest group, and 91 MAGs to the cropland group. Metabolic networks were constructed and visualized using R. MAGs exhibiting both co-occurrence properties (from the co-occurrence network) and metabolic cooperation potential (from the $MI_{Complementarity}$ network)

were classified as “dual interactions”.

The potential exchangeable metabolites under mutualistic interactions were identified following the approach outlined by Peng et al. (2024). Specifically, for a given MAG pair, when a metabolite was found in the seed set of MAG A but not in that of MAG B, this pattern was interpreted as indicating a potential transfer from MAG B to MAG A. In this case, MAG B was considered the potential donor, as it was inferred to be able to synthesize the metabolite, whereas MAG A was considered the potential recipient, as it was inferred to utilize the metabolite. Metabolite profiles were derived from genome-scale metabolic models generated using CarveMe and the BiGG Model database (version 1.6). Metabolites were classified at the “super class” level using the Human Metabolome Database (HMDB, version 5.0), into five categories: coenzyme A derivatives; amino acids, peptides, and analogs; carbohydrates and carbohydrate conjugates; nucleosides, nucleotides, and analogs; and other metabolites. A map of potentially transferable metabolites was constructed based on the direction of metabolite transfer.

2.6 Statistical analyses

Functional diversity of CAZymes, COGs, and KOs was estimated using the *vegan* package. Similarity of CAZyme, COG, and KO functional gene composition were calculated with the *vegdist* function based on Bray-Curtis dissimilarity. Paired t-tests to assess significant differences were conducted using SPSS 25.0 (IBM Inc., Armonk, NY). Bar and box plots were generated using the *ggplot2* package. Spearman’s correlation coefficient was used to assess associations between environmental factors and microbial functions in heat maps. Regression analysis was performed using linear or quadratic models using the *ggplot2* package. Principal coordinate analysis (PCoA) was applied to examine the dissimilarity in microbial community structure of CAZymes, COGs, and KOs between forest and cropland. Permutational multivariate analysis of variance (PERMANOVA), based on Bray-Curtis dissimilarity with 999 permutations, was used to compare microbial community differences between forest and cropland, performed via the *adonis2* function in the *vegan* package. Because forest and cropland samples were paired on the same bank within each sampling location, this forest–cropland pairing structure was accounted for in the PERMANOVA analysis to control for non-

independence among paired samples. ARG diversity and high-risk ARG abundance were calculated using the same method as microbial functional diversity. Distance between sampling sites was calculated as the cumulative sum of distances from each site to the next, starting from the first and ending at the last.

The influences on ARG diversity and microbial functions in forest and cropland soils, as well as the path relationships between these factors and normalized environmental variables, were examined using structural equation modeling (SEM). Model fit was assessed using the following indices: CFI > 0.90, RMSEA < 0.1, $p > 0.05$, and $\chi^2/df < 5$. Separate SEMs were constructed for forest soils and cropland soils rather than fitting a single joint model across both land use types. The SEM included a range of environmental factors: geographic (distance from the upper Yangtze River), climatic (mean annual temperature and precipitation), plant (richness of arbores, shrubs, and herbs; litter dry weight), soil (soil moisture, pH, organic carbon, total nitrogen, total phosphorus, NH_4^+-N, soil enzymes), biological (average genome size, 16S rRNA copy number), social (population, GDP per capita, agricultural GDP per capita, grain output per unit area, fertilizer and pesticide use per unit area) factors, microbial metabolism (complementary and competitive interactions), CAZyme similarity, and microbial functions. Social factors were additionally included as contextual exploratory covariates reflecting regional differences in human activity intensity and agricultural management. Microbial complementarity was calculated by multiplying normalized MAG abundance, $MI_{Complementarity}$, and node degree in the complementary network, while microbial competition was determined by multiplying normalized MAG abundance, $MI_{Competition}$, and node degree in the competition network. Environmental heterogeneity was assessed by performing PCoA on variables including mean annual temperature, precipitation, soil moisture, pH, organic carbon, total nitrogen, total phosphorus, and NH_4^+-N, followed by Euclidean distance computation between points based on their PCo1 and PCo2 coordinates.

3. Results

3.1 Microbial CAZyme genes and ARGs in forest and cropland soils

Land-use change increased CAZyme gene similarity in cropland soils compared to forest

soils ($p < 0.01$; Fig. 1B). CAZyme gene similarity in forest soils showed a stronger quadratic relationship with the distance from the upper Yangtze River ($R^2 = 0.307$, $p < 0.001$) than in cropland soils ($R^2 = 0.069$, $p = 0.002$; Fig. 1C). Land-use change decreased CAZyme gene diversity in cropland soils ($p < 0.05$; fig. S1), including specific genes involved in glycoside hydrolases (e.g., GH76, GH66, GH116) and carbohydrate-binding modules (e.g., CBM42). PCoA revealed distinct CAZyme gene compositions between forest and cropland soils (PERMANOVA, $p < 0.001$). Land-use change also increased similarity of COG functional gene composition ($p < 0.05$), and PCoA showed significant compositional separation between the two soil types (fig. S2).

Land-use change from forest to cropland increased the average ARG diversity by 35.6% in soils (Fig. 1E), with higher diversity near the upper Yangtze River (Fig. 1F). ARG subtypes related to tetracycline, beta-lactam, and macrolide-lincosamide-streptogramin (MLS) were significantly enriched in cropland soils ($p < 0.001$; Fig. 1G). ARG abundance was higher close to the upper Yangtze River, and high-risk ARGs, including *bacA*, *mexD*, *sul1*, and *sul2*, were significantly more abundant in cropland soils ($p < 0.001$; fig. S3).

3.2 Microbial life history strategies and traits in forest and cropland soils

Multivariate co-inertia analysis (MCOA) identified two key dimensions explaining 43.56% (MCOA1) and 15.50% (MCOA2) of the variation in microbial community-aggregated traits (CATs) (Fig. 2A), highlighting distinct life history strategies in forest and cropland soils. MCOA1 showed differences in nutrient recycling and metabolic capacity, with forest soil microbial communities clustering at the right end of the axis, exhibiting greater metabolic capacity. While cropland soil microbial communities clustered at the left end of the axis, showing higher nutrient recycling potential (Figs. 2A, S4). Forest soil microbial communities had a significantly larger average genome size ($p < 0.001$) and a higher abundance of genes related to membrane synthesis and repair ($p < 0.001$; Figs. 2B, 2C). MCOA2 reflected environmental responsiveness, with cropland soil microbial communities clustering at the upper end of the axis, indicating greater adaptability (Figs. 2A, S4). Cropland soil microbial communities had a significantly larger average 16S rRNA gene copy number ($p < 0.001$) and a higher abundance of genes involved in amino acid, fatty acid, and nucleotide synthesis ($p <$

0.001), chemotaxis ($p < 0.01$), and exoenzyme production ($p < 0.05$; Figs. 2D-G).

To further distinguish microbial functional traits between forest and cropland soils, metagenomic binning analysis was performed and identified 114 high-quality metagenome-assembled genomes (MAGs) (> 90% completeness, < 5% contamination) (Fig. 3). Most MAGs belonged to Acidobacteria, Proteobacteria, and Thermoproteota, with genome sizes ranging from 1.19 Mb to 8.88 Mb. The largest microbial genome (*S121C11140*), affiliated with Actinobacteriota, was primarily found in forest soils. MAG abundance varied significantly between the two ecosystems, with Acidobacteriota-affiliated MAGs *S77C1406* and *S78C6383* more abundant in cropland soils, while Proteobacteria-affiliated MAG *S228C2606* dominated forest soils ($p < 0.05$). Cropland-dominant MAGs exhibited lower CAZyme gene diversity but higher ARG diversity than those in forest soils. For example, forest soil MAG *S121C11140* had the highest number (35) of CAZyme genes (35), dominated by glycoside hydrolase and glycosyl transferase genes, whereas cropland soil MAG *S75C15731* (Proteobacteria) showed the highest number (62) of ARGs, primarily associated with multidrug resistance.

3.3 Microbial metabolic interaction networks in forest and cropland soils

To corroborate the effects of land-use change on microbial interactions, we constructed co-occurrence networks of microbial communities in forest and cropland soils (fig. S6). The networks of both soil types were dominated by positive correlations between microbial nodes. The forest soil microbial network had higher density, shorter path length, greater clustering coefficient, and lower modularity than the cropland soil microbial network (Table S1), indicating more tightly connected microbial interactions in forest soils.

We constructed GSMMs to assess microbial metabolic dependencies in forest and cropland soils. Using PhyloMint indices, we quantified microbial metabolic complementarity ($MI_{complementarity}$) and competition ($MI_{competition}$) between MAG pairs. Mutualistic interactions were more prevalent in forest soils (4.5%) than in cropland soils (3.2%), whereas competitive interactions were more frequent in cropland soils (2.3%) than in forest soils (1.8%) (Figs. S7, S8). Commensal interactions (where $MI_{complementarity}$ exceeded the threshold for one MAG) were more common in forest soils (36.7%) than in cropland soils (32.5%) (Figs. 4A, 4B), while amensal interactions (where $MI_{competition}$ exceeded the threshold for one MAG) were more

frequent in cropland soils (8.3%) than in forest soils (5.7%), increased by 45.6% (Figs. 4C, 4D). The metabolic complementarity network in forest soils had higher clustering and density, but shorter path length than that in cropland soils (Table S2). Whereas the metabolic competition network in cropland soils exhibited higher values of these properties than that in forest soils (Table S3). Pairwise $MI_{complementarity}$ values were higher in forest soils ($p < 0.001$; Fig. 4E), while $MI_{competition}$ values were higher in cropland soils ($p < 0.001$; Fig. 4G). Moreover, $MI_{complementarity}$ increased with microbial genome size differences (Δsize) between MAG pairs, whereas $MI_{competition}$ decreased (Figs. 4F, 4H), with greater variation observed in cropland soils. In cropland soils, MAGs with higher growth ratios were more frequently associated with higher ARG diversity categories (Fig. 4I). Likewise, MAGs with higher $MI_{competition}$ values were more often linked to higher ARG diversity categories (Fig. 4J).

In the metabolic cooperative networks, we identified reliable metabolite transfer pathways, illustrating the complexity of microbial metabolic traits through interactions between archaea and bacteria. Microbial genome size differences (Δsize) and metabolic traits were supported by both metabolic and co-occurrence networks, highlighting key MAGs with significant metabolic cooperative relationships in forest and cropland soils. In forest soils, the archaeal MAG *S130C426* (Thermoproteota) formed mutualistic interactions with six bacterial partners, primarily from Eremiobacterota and Acidobacteria (Fig. 5A). Serving as a central metabolic hub, *S130C426* supplied carbohydrates to its bacterial partners while receiving coenzymes, maintaining a balanced exchange of essential metabolites. In cropland soils, *S130C426* engaged in fewer mutualistic interactions, partnering with four bacterial MAGs, including Bacteroidota and Eremiobacterota (Fig. 5B). Although amino acids and carbohydrates were still exchanged, their diversity, quantity, and frequency were lower than in forest soils, indicating reduced metabolic interdependence in cropland soils.

3.4 Associations between soil carbon metabolic homogenization and ARG diversity

SEMs were used to assess the relationships among multiple environmental and biological factors influencing microbial metabolism, CAZyme gene similarity, and ARG diversity in forest and cropland soils across the Yangtze River Basin. The models incorporated geographic factors (distances from the upper Yangtze River), climatic variables (mean annual temperature and

precipitation), socioeconomic indicators in croplands (total population, GDP, cropland production, grain output, and fertilizer/pesticide use), plant factors in forests (arbor, shrub, and herb richness, as well as litter dry weight), soil properties (moisture, pH, organic carbon, total nitrogen, total phosphorus, NH_4^+-N, and enzyme activity), and microbial traits (genome size and 16S rRNA gene copy number).

CAZyme gene similarity was a key determinant of ARG diversity across ecosystems but exhibited contrasting roles in forest and cropland soils. In forest soils, CAZyme gene similarity had a direct and significant positive effect on ARG diversity (standardized total effect: 0.33; r = 0.33; $p < 0.01$; Fig. 6A, fig. S10), whereas in cropland soils, its effect was indirect, mediated via the shifts of microbial metabolic competition (Fig. 6C). In forests, soil factors positively regulated microbial metabolic complementarity, while biological factors exerted a negative influence (Fig. 6A). By contrast, in croplands, CAZyme gene similarity was significantly associated with land-use change (r = 0.33; fig. S9). Microbial metabolic interactions played divergent roles in shaping ARG diversity. In forests, CAZyme gene similarity and biological factors (standardized total effects: 0.33 and -0.21, respectively) were strong predictors of ARG diversity, whereas climatic factors had negligible impacts (Fig. 6B). Conversely, in croplands, competition had a positive effect (Fig. 6D), with microbial metabolism acting as the dominant driver. Social factors showed no significant direct effect on ARG diversity (r = 0.09, $p = 0.22$). However, in the cropland SEM, the composite social factor showed an overall negative association with ARG diversity (standardized total effect = –0.19) and a weak overall positive association with microbial competition (standardized total effect = 0.04). Notably, microbial genome traits were also associated with ARG patterns that genome size showed a negative correlation but 16S rRNA gene copy number showed a positive correlation with ARG diversity (fig. S10).

CAZyme gene similarity was negatively correlated with environmental heterogeneity in both forests and croplands ($p < 0.001$; fig. S11), with a steeper decline in forest soils (S = -0.165) than in cropland soils (S = -0.105). SEM results identified soil factors as the primary regulators of CAZyme gene diversity and microbial life history traits (MCOA1 and MCOA2) in both ecosystems (fig. S12). Additionally, distance from the dam negatively impacted

CAZyme gene diversity in forest soils (-0.19), while biological factors strongly and negatively influenced MCOA2 in cropland soils (-0.873).

4. Discussion

Here, we propose a conceptual framework in which carbon metabolic homogenization associated with land-use change may intensify microbial competition for metabolites and, in turn, contribute to higher ARG diversity, including high-risk ARGs (Fig. 7). This framework summarizes our key findings by linking land-use change with shifts in microbial functional traits and metabolite interaction networks. Specifically, our results suggest that land-use change is associated with increased carbon metabolic homogenization, which selects for microbial taxa with streamlined genomes and narrower metabolic repertoires. These adaptations increase competitive pressures within microbial communities, thereby favoring the emergence and persistence of ARGs.

4.1 Carbon metabolic homogenization and ARG increase under land-use change

We found significantly higher microbial CAZyme gene similarity in cropland soils than in forest soils, suggesting that intensive management practices such as tillage, fertilization, and pesticide application lead to microbial carbon functional homogenization [49]. This pattern often associates with the reductions in plant diversity, vegetation cover, and biomass production under land-use change from forest to cropland, which diminish the diversity and complexity of organic matter inputs [50,51]. Glycosyl transferase genes, which contribute to glycosylation of secondary metabolites and complex molecule synthesis [52], are enriched in forest soils. Cropland soils, in contrast, show elevated levels of glycoside hydrolase genes, reflecting an adaptation toward simpler carbohydrate breakdown under homogenized input conditions [2]. This shift in CAZyme composition underlines the constrained carbon source range in croplands and the decreased microbial functional diversity, indicating diminished ecosystem buffering capacity and functional stability under land-use change [53].

In parallel, ARG diversity was significantly increased under land-use change, suggesting that agricultural activities such as livestock manure result in the increase of ARGs in cropland soils [54]. In addition, cropland soils may be more frequently exposed to wastewater related

contaminants and residual agrochemicals, including fertilizers and pesticides, which can further impose selective pressures that favor the maintenance and enrichment of ARGs [55]. Such conditions may also promote the mobility of resistance determinants through horizontal gene transfer, thereby facilitating ARG dissemination within agricultural microbial communities [56]. Moreover, the abundance of high-risk ARGs was also increased under land-use change, highlighting higher ecological and human health risks in cropland soils. For example, *sul1* confers resistance to sulfonamide which is one of the most widely used antibiotics in clinical care [57], while *mexD* diminishes the efficacy of a broad spectrum of antibiotics and can contribute to the emergence of multidrug-resistant pathogens that will compromise public health [58]. Previous study from agricultural soils in the Yangtze River region have further shown that total nitrogen content is positively correlated with *sul1* abundance, suggesting that anthropogenic nitrogen fertilization in cropland soils may contribute to the persistence and enrichment of resistance determinants . Horizontal gene transfer of ARGs is widely recognized as a major pathway for the dissemination of antibiotic resistance [59]. Integrons are important MGEs that contribute to the capture, mobilization, and spread of ARGs among bacterial taxa. Among them, previous study has also reported a positive association between MGEs and *sul1*, suggesting that the enrichment of sul1 may be closely linked to MGE mediated horizontal transfer [60]. Overall, land-use change expands soil ARG diversity and amplifies high-risk ARGs, intensifying potential risks to public health.

4.2 Microbial life strategies alteration to adapt to carbon metabolic homogenization

The alteration of microbial carbon metabolic function under land-use change is closely associated with the choice of different microbial life strategies. Our results revealed that forest soils harbored microbes with a larger genomic size that can encode a wider array of functional genes, showing a greater functional complexity compared to cropland soils. This life strategy supports microbes in forest soils to encode diverse types of carbon metabolic genes that can facilitate the utilization of heterogeneous and complex carbon source inputs such as plant litter and debris [61]. While a great number of genes involved in membrane synthesis and repair can safeguard microbial cellular integrity under disturbance and stress to steadily utilize these carbon sources [62]. These key functional traits confer a higher ecological advantage in

adapting to complex carbon source inputs, enabling resource flexibility and resistance to environmental changes. The functional repertoire is consistent with the "red queen hypothesis" [63], whereby microbial communities maintain a broad set of costly yet essential functions, enhancing metabolic capacity under environmental changes.

In contrast, agricultural practices favor fast-growing microbes with small genomes and streamlined metabolic strategies. The loss of non-essential metabolic functional genes through genome reduction constrains the capacity to exploit diverse carbon sources, but enables more efficient use of readily available inputs, thereby accelerating microbial growth rates. This life strategy is supported by the "black queen hypothesis" that genome reduction and streamlining can confer adaptive advantages under environmental stress by minimizing metabolic burdens and reallocating resources toward rapid proliferation [64,44]. Moreover, we observed an enrichment of genes involved in amino acid, fatty acid, and nucleotide synthesis in cropland soils, suggesting that microbes tend to engage in traits with great metabolic self-sufficiency and rapid growth to adapt to specialized carbon source inputs and metabolic homogenization [65]. Our results highlight the impact of land-use change on microbial ecological strategies, showing that cropland practices favor specialized and fast-growing microbes that are efficient in nutrient cycling but lack the metabolic flexibility to utilize diverse carbon sources. Although genome based microbial taxonomy continues to be updated and some MAG assignments may be refined in future GTDB releases, particularly at lower taxonomic ranks, the ecological interpretations in this study rely primarily on broad taxonomic patterns and are therefore unlikely to be substantially altered by such updates.

4.3 Intensified competition within microbial communities raises ARG diversity

Our results indicated that land-use change altered the structure of microbial interaction networks. Microbial community exhibited stronger cooperative interactions and higher metabolic complementarity in forest soils, as evidenced by our transferable metabolite analysis. In forest soils, high metabolic diversity facilitates microbial niche differentiation and metabolite sharing [26], giving rise to interaction networks characterized by phylogenetic and functional diversity that enable microbial cooperation even across domains (e.g., bacteria and archaea). For instance, Thermoproteota formed more cooperative associations with bacteria such as

Eremiobacterota and Acidobacteria, engaging in metabolite exchange with diverse microbial partners. This is consistent with genome-based differentiation, where larger-genome microbes usually serve as metabolite providers, while smaller-genome microbes act as recipients and benefit from complementary functions, representing an ecological labor division that enhances the metabolic efficiency within microbial community. Such metabolite exchange reduces the metabolic burden on individual microbes, promotes resource complementarity, and stabilizes community function under fluctuating environmental conditions.

By contrast, microbial community displayed fewer cooperative interactions and metabolic functions in cropland soils, indicating a weakness of functional complementarity. Metabolic network analyses indicated that competitive relationships were predominantly concentrated among closely related bacteria, as phylogenetically similar taxa occupy overlapping ecological niches that can intensify resource competition [66]. Under antibiotic pressure, microorganisms carrying ARGs may become more competitive and gradually replace taxa that originally occupied the same niches [67]. On the other hand, carbon metabolic homogenization in cropland soils intensifies microbial competition for nutrient inputs, where rapid growth and nutrient cycling drive microbes to secrete antibiotics to suppress their competitors [68], thereby fostering higher ARG diversity. Under resource-limited conditions, ARG-carrying microorganisms may gain a selective advantage beyond resistance. ARGs are often embedded in broader adaptive genetic backgrounds, including mobile genetic elements and stress-related functions. For example, resistance determinants may co-occur with efflux, membrane protection, and chemical tolerance functions [69]. Microbial rapid growth can also increase the frequence of horizontal gene transfer to accelerate ARG spread [70]. This interpretation was further supported by the MAG level analysis in cropland soils, where MAGs with higher growth ratios and higher $MI_{competition}$ values were more often associated with higher ARG diversity categories. This result provides additional support that the fast growing and more competitive taxa in cropland soils may represent important hosts of enriched ARGs. Together, our study supports the hypothesis that carbon homogenization associated with land use change contribute to higher ARG diversity through changes in microbial interactions, highlighting the need to integrate microbial functional traits and interaction networks into ARG health risk assessment.

As this study was based on large scale field observations, the relationships identified here should be interpreted as patterns of association rather than direct causal effects. Further experimental and longitudinal studies will help to test the proposed mechanisms more directly.

5. Conclusion

This study shows that land-use change from forests to croplands across the Yangtze River Basin was associated with greater carbon metabolic homogenization, stronger predicted microbial competition for metabolites, and higher soil ARG diversity. We propose a conceptual framework linking microbial life history traits, interaction networks, and ARG diversity, suggesting that land use change may be associated with a shift in microbial communities from more cooperative to more competitive interaction patterns, together with higher ARG diversity. Our genome-scale metabolic models provide evidence that carbon metabolic homogenization altered microbial interactions from cooperation to competition, with fewer metabolite exchanges in cropland soils, as revealed by our metabolite transfer network analyses. The alteration was accompanied by a shift from large-genome and functionally diverse microbes to fast-growing and competition-adapted microbes with limited metabolic complementarity in cropland soils. These findings highlight the need for agricultural management strategies that help preserve microbial functional diversity, including maintaining more diverse agricultural systems, reducing prolonged land use simplification, and more carefully managing organic matter inputs to help limit ARG proliferation.

6. Environmental Implication

Agricultural expansion reshaped soil microbial communities toward competition-dominated, resource-acquisitive strategies and higher ARG diversity through carbon metabolic homogenization. This study identifies a microbial interaction pathway linking land-use intensification to antimicrobial resistance risks, providing an ecological basis for land management strategies that protect soil health and support One Health goals.

Acknowledgments

This work was financially supported by the National Key Research and Development Program of China (2024YFE0106300), National Natural Science Foundation of China

(42307033 and U25A20803), Fujian Provincial Natural Science Foundation China (2023J02031), Strategic Priority Research Program of Chinese Academy of Sciences (XDA28020101), UK Research and Innovation (MR/Y015223/1), and Ningbo Yongjiang Talent Project (2022-163-G).

Author contributions

S.-Y.Z. and T.-L.Z. conceived the study, performed formal analyses, prepared visualizations, and drafted the manuscript. S.D. contributed to conceptualization, methodology, supervision, funding acquisition, and manuscript revision. Z.-G.Y. revised the manuscript and acquired funding. S.-E.L. acquired funding, provided supervision, methodology support, and manuscript revision. G.-Y.Z. contributed methodology and manuscript revision. M.D.-B. contributed to conceptualization, ecological interpretation, and manuscript revision. D.Z. conceived the study, supervised the project, acquired funding, drafted, and revised the manuscript. All authors read and approved the final manuscript.

Conflicts of Interest

The authors declare that they have no competing interests.

References

[1] Liu, L., Wang, H., Guo, Y., Yan, Q., Chen, J., 2024. Human-induced homogenization of microbial taxa and function in a subtropical river and its impacts on community stability, Water Res. 252, 121198. https://doi.org/10.1016/j.watres.2024.121198.

[2] Xu, Q., Zhang, H., Vandenkoornhuyse, P., Guo, S., Kuzyakov, Y., Shen, Q., Ling, N., 2024. Carbon starvation raises capacities in bacterial antibiotic resistance and viral auxiliary carbon metabolism in soils, Proc. Natl. Acad. Sci. 121, e2318160121. https://doi.org/doi:10.1073/pnas.2318160121.

[3] Zhou, X., Liu, S., Wang, B., Wu, L., Wu, Y., Zhang, H., Chen, D., 2025. Forest conversion-induced soil biota homogenization destabilizes ecosystem functions, Commun. Earth Environ. 6, 882. https://doi.org/10.1038/s43247-025-02909-7.

[4] FAO, 2009. Global Agriculture towards 2050. Rome.

[5] Potapov, P., Turubanova, S., Hansen, M.C., Tyukavina, A., Zalles, V., Khan, A., Song, X.-P., Pickens, A., Shen, Q., Cortez, J., 2022. Global maps of cropland extent and change show accelerated cropland expansion in the twenty-first century, Nat. Food 3, 19-28. https://doi.org/10.1038/s43016-021-00429-z.

[6] Lin, D., Liu, Y., Liu, X., Du, S., Leung, K.M.Y., Zhu, Y.-G., Wu, F., Zhu, D., 2026. Urban wetlands as hotspots of antibiotic resistomes and their potential viral transmission, Nat. Cities. https://doi.org/10.1038/s44284-026-00433-z.

[7] Tan, L., Li, H., Xu, Y., 2026. Socioeconomic Factors Influence Human Exposure to Antibiotic Resistance Genes in Rural Surface Waters of the Yangtze River Basin, Agricultural Environment and Sustainability, 100017. https://doi.org/https://doi.org/10.1016/j.ages.2026.100017.

[8] Wang, J., Zhu, Y.-G., Ge, Y., 2024. Global distribution pattern of soil phosphorus-cycling microbes under the influence of human activities, Global Change Biol. 30, e17477. https://doi.org/https://doi.org/10.1111/gcb.17477.

[9] Nepal, D., Parajuli, P.B., Ouyang, Y., To, S.D.F., Wijewardane, N., 2023. Assessing hydrological and water quality responses to dynamic landuse change at watershed scale in Mississippi, J. Hydrol. 625, 129983. https://doi.org/10.1016/j.jhydrol.2023.129983.

[10] Battin, T.J., Lauerwald, R., Bernhardt, E.S., Bertuzzo, E., Gener, L.G., Hall Jr, R.O., Hotchkiss, E.R., Maavara, T., Pavelsky, T.M., Ran, L., Raymond, P., Rosentreter, J.A., Regnier, P., 2023. River ecosystem metabolism and carbon biogeochemistry in a changing world, Nature 613, 449-459. https://doi.org/10.1038/s41586-022-05500-8.

[11] Varis, O., Taka, M., Kummu, M., 2019. The Planet's Stressed River Basins: Too Much Pressure or Too Little Adaptive Capacity?, Earths Future 7, 1118-1135. https://doi.org/10.1029/2019ef001239.

[12] Jimenez, R., Ardila, A.V., Vargas-Burbano, A.C., Hernandez, A.J., Leon-Velasquez, E., 2022. Biomass burning-agriculture coupling in the Orinoco savannas—Particulate matter emission scenarios, Front. Environ. Sci. Volume 10 - 2022. https://doi.org/10.3389/fenvs.2022.689844.

[13] InfoAmazonia, 2023. Deforestation in the Amazon: Past, present and future. https://infoamazonia.org/en/2023/03/21/deforestation-in-the-amazon-past-present-and-future/.

[14] Peng, Z.H., Qian, X., Liu, Y., Li, X.M., Gao, H., An, Y.N., Qi, J.J., Jiang, L., Zhang, Y.R., Chen, S., Pan, H.B., Chen, B.B., Liang, C.L., van der Heijden, M.G.A., Wei, G.H., Jiao, S., 2024. Land conversion to agriculture induces taxonomic homogenization of soil microbial communities globally, Nat. Commun. 15, 3624. https://doi.org/10.1038/s41467-024-47348-8.

[15] Lemos, L.N., Pedrinho, A., de Vasconcelos, A.T.R., Tsai, S.M., Mendes, L.W., 2021. Amazon deforestation enriches antibiotic resistance genes, Soil Biol. Biochem. 153. https://doi.org/10.1016/j.soilbio.2020.108110.
[16] Jin, L., Pruden, A., Boehm, A.B., Alvarez, P.J.J., Raskin, L., Kohn, T., Li, X., 2022. Integrating Environmental Dimensions of "One Health" to Combat Antimicrobial Resistance: Essential Research Needs, Environ. Sci. Technol. 56, 14871-14874. https://doi.org/10.1021/acs.est.2c01651.
[17] Yan, Z., Kang, E., Zhang, K., Hao, Y., Wang, X., Li, Y., Li, M., Wu, H., Zhang, X., Yan, L., Zhang, W., Li, J., Yang, A., Niu, Y., Kang, X., 2022. Asynchronous responses of microbial CAZymes genes and the net CO2 exchange in alpine peatland following 5 years of continuous extreme drought events, ISME Commun. 2, 115. https://doi.org/10.1038/s43705-022-00200-w.
[18] Zhao, Z., Baltar, F., Herndl, G.J., 2020. Linking extracellular enzymes to phylogeny indicates a predominantly particle-associated lifestyle of deep-sea prokaryotes, Sci. Adv. 6. https://doi.org/10.1126/sciadv.aaz4354.
[19] Dou, P., Wang, J., Cai, T., Miao, Z., Wang, X., Liang, J., Li, P., Fan, J., Tang, S., Xiao, X., Guo, L., Huang, J., Gao, Q., Chen, C., Liu, K., Wang, K., 2025. Influence of Initial Soil Organic Carbon in Grassland on the Sensitivity of Carbon Changes to Climate After Grassland-to-Cropland Conversion, Earth's Future 13, e2024EF005249. https://doi.org/https://doi.org/10.1029/2024EF005249.
[20] Li, Z., Shangguan, H., Yao, H., Yang, X., Mazei, Y., Zhu, B., Scheu, S., Sun, X., 2024. Colonization ability and uniformity of resources and environmental factors determine biological homogenization of soil protists in human land-use systems, Global Change Biol. 30, e17411. https://doi.org/10.1111/gcb.17411.
[21] Allen, H.K., Donato, J., Wang, H.H., Cloud-Hansen, K.A., Davies, J., Handelsman, J., 2010. Call of the wild: antibiotic resistance genes in natural environments, Nat. Rev. Microbiol. 8, 251-259. https://doi.org/10.1038/nrmicro2312.
[22] Dibner, J.J., Richards, J.D., 2005. Antibiotic growth promoters in agriculture: History and mode of action, Poult. Sci. 84, 634-643. https://doi.org/10.1093/ps/84.4.634.
[23] Gu, C., Kim, G.B., Kim, W.J., Kim, H.U., Lee, S.Y., 2019. Current status and applications of genome-scale metabolic models, Genome Biol. 20, 121. https://doi.org/10.1186/s13059-019-1730-3.
[24] Zelezniak, A., Andrejev, S., Ponomarova, O., Mende, D.R., Bork, P., Patil, K.R., 2015. Metabolic dependencies drive species co-occurrence in diverse microbial communities, Proceedings of the National Academy of Sciences 112, 6449-6454. https://doi.org/doi:10.1073/pnas.1421834112.
[25] Wang, W., Xia, Y., Zhang, P., Zhu, M., Huang, S., Sun, X., Xu, Z., Zhang, N., Xun, W., Shen, Q., Miao, Y., Zhang, R., 2025. Narrow-spectrum resource-utilizing bacteria drive the stability of synthetic communities through enhancing metabolic interactions, Nat. Commun. 16, 6088. https://doi.org/10.1038/s41467-025-61432-7.
[26] Peng, X., Wang, S., Wang, M., Feng, K., He, Q., Yang, X., Hou, W., Li, F., Zhao, Y., Hu, B., Zou, X., Deng, Y., 2024. Metabolic interdependencies in thermophilic communities are revealed using co-occurrence and complementarity networks, Nat. Commun. 15, 8166. https://doi.org/10.1038/s41467-024-52532-x.
[27] Zhan, C., Yang, Y., Wu, X., Jiang, Y., 2024. Spatial-Temporal Variations of the Water Quality and the Pollutants Sources in the Yangtze River (Hubei Province), Water Resour. 51, 1054-1064. https://doi.org/10.1134/s0097807823601590.
[28] Gao, Y., Zhang, W.L., Li, Y., Wu, H.N., Yang, N., Hui, C.Z., 2021. Dams shift microbial

community assembly and imprint nitrogen transformation along the Yangtze River, Water Res. 189, 11579. https://doi.org/10.1016/j.watres.2020.116579.
[29] Huang, S., Shah, H., Naz, B.S., Shrestha, N., Mishra, V., Daggupati, P., Ghimire, U., Vetter, T., 2020. Impacts of hydrological model calibration on projected hydrological changes under climate change-a multi-model assessment in three large river basins, Clim. Change 163, 1143-1164. https://doi.org/10.1007/s10584-020-02872-6.
[30] Xu, Y.Q., Hou, R.P., Xiao, F.J., 2024. Ecosystem services in the Yangtze River Basin and their trade-offs/synergies relationships in response to climate change, Environ. Res. Commun. 6, 105032. https://doi.org/10.1088/2515-7620/ad8057.
[31] Zhou, X., Cai, J., Xu, J., Liu, S., Wang, B., Zhang, H., Yue, L., Wu, L., Wu, Y., Chen, D., 2024. Climate regulates the effect of land-use change on the diversity of soil microbial functional groups and soil multifunctionality, J. Appl. Ecol. 61, 2087-2099. https://doi.org/10.1111/1365-2664.14722.
[32] Bian, R., Huang, S., Cao, X., Qi, W., Peng, J., Liu, H., Wu, X., Li, C., Qu, J., 2024. Spatial and temporal distribution of the microbial community structure in the receiving rivers of the middle and lower reaches of the Yangtze River under the influence of different wastewater types, J. Hazard. Mater. 462, 132835. https://doi.org/10.1016/j.jhazmat.2023.132835.
[33] Wang, B., Wu, L.J., Chen, D.M., Wu, Y., Hu, S.J., Li, L.H., Bai, Y.F., 2020. Grazing simplifies soil micro-food webs and decouples their relationships with ecosystem functions in grasslands, Global Change Biol. 26, 960-970. https://doi.org/10.1111/gcb.14841.
[34] Wagg, C., Bender, S.F., Widmer, F., van der Heijden, M.G.A., 2014. Soil biodiversity and soil community composition determine ecosystem multifunctionality, Proc. Natl. Acad. Sci. 111, 5266-5270. https://doi.org/10.1073/pnas.1320054111.
[35] Alneberg, J., Bjarnason, B.S., de Bruijn, I., Schirmer, M., Quick, J., Ijaz, U.Z., Lahti, L., Loman, N.J., Andersson, A.F., Quince, C., 2014. Binning metagenomic contigs by coverage and composition, Nat. Methods 11, 1144-1146. https://doi.org/10.1038/nmeth.3103.
[36] Bowers, R.M., Kyrpides, N.C., Stepanauskas, R., Harmon-Smith, M., Doud, D., Reddy, T.B.K., Schulz, F., Jarett, J., Rivers, A.R., Eloe-Fadrosh, E.A., Tringe, S.G., Ivanova, N.N., Copeland, A., Clum, A., Becraft, E.D., Malmstrom, R.R., Birren, B., Podar, M., Bork, P., Weinstock, G.M., Garrity, G.M., Dodsworth, J.A., Yooseph, S., Sutton, G., Gloeckner, F.O., Gilbert, J.A., Nelson, W.C., Hallam, S.J., Jungbluth, S.P., Ettema, T.J.G., Tighe, S., Konstantinidis, K.T., Liu, W.-T., Baker, B.J., Rattei, T., Eisen, J.A., Hedlund, B., McMahon, K.D., Fierer, N., Knight, R., Finn, R., Cochrane, G., Karsch-Mizrachi, I., Tyson, G.W., Rinke, C., Lapidus, A., Meyer, F., Yilmaz, P., Parks, D.H., Eren, A.M., Schriml, L., Banfield, J.F., Hugenholtz, P., Woyke, T., Genome Stand, C., 2017. Minimum information about a single amplified genome (MISAG) and a metagenome-assembled genome (MIMAG) of bacteria and archaea, Nat. Biotechnol. 35, 725-731. https://doi.org/10.1038/nbt.3893.
[37] Rodríguez del Río, Á., Scheu, S., Rillig, M.C., 2025. Soil microbial responses to multiple global change factors as assessed by metagenomics, Nat. Commun. 16, 5058. https://doi.org/10.1038/s41467-025-60390-4.
[38] Parks, D.H., Rinke, C., Chuvochina, M., Chaumeil, P.-A., Woodcroft, B.J., Evans, P.N., Hugenholtz, P., Tyson, G.W., 2017. Recovery of nearly 8,000 metagenome-assembled genomes substantially expands the tree of life, Nat. Microbiol. 2, 1533-1542. https://doi.org/10.1038/s41564-017-0012-7.
[39] Yin, X., Zheng, X., Li, L., Zhang, A.-N., Jiang, X.-T., Zhang, T., 2023. ARGs-OAP v3.0:

Antibiotic-resistance gene database curation and analysis pipeline optimization, Engineering 27, 234-241. https://doi.org/https://doi.org/10.1016/j.eng.2022.10.011.
[40] Zhang, Z., Zhang, Q., Wang, T., Xu, N., Lu, T., Hong, W., Penuelas, J., Gillings, M., Wang, M., Gao, W., Qian, H., 2022. Assessment of global health risk of antibiotic resistance genes, Nat. Commun. 13, 1553. https://doi.org/10.1038/s41467-022-29283-8.
[41] Bahram, M., Hildebrand, F., Forslund, S.K., Anderson, J.L., Soudzilovskaia, N.A., Bodegom, P.M., Bengtsson-Palme, J., Anslan, S., Coelho, L.P., Harend, H., Huerta-Cepas, J., Medema, M.H., Maltz, M.R., Mundra, S., Olsson, P.A., Pent, M., Polme, S., Sunagawa, S., Ryberg, M., Tedersoo, L., Bork, P., 2018. Structure and function of the global topsoil microbiome, Nature 560, 233-237. https://doi.org/10.1038/s41586-018-0386-6.
[42] Lombard, V., Ramulu, H.G., Drula, E., Coutinho, P.M., Henrissat, B., 2014. The carbohydrate-active enzymes database (CAZy) in 2013, Nucleic Acids Res. 42, D490-D495. https://doi.org/10.1093/nar/gkt1178.
[43] Pereira-Flores, E., Gloeckner, F.O., Fernandez-Guerra, A., 2019. Fast and accurate average genome size and 16S rRNA gene average copy number computation in metagenomic data, BMC Bioinf. 20, 453. https://doi.org/10.1186/s12859-019-3031-y.
[44] Piton, G., Allison, S.D., Bahram, M., Hildebrand, F., Martiny, J.B.H., Treseder, K.K., Martiny, A.C., 2023. Life history strategies of soil bacterial communities across global terrestrial biomes, Nat. Microbiol. 8, 2093-2102. https://doi.org/10.1038/s41564-023-01465-0.
[45] Meng, C., Kuster, B., Culhane, A.C., Gholami, A.M., 2014. A multivariate approach to the integration of multi-omics datasets, BMC Bioinf. 15, 162. https://doi.org/10.1186/1471-2105-15-162.
[46] Feng, K., Peng, X., Zhang, Z., Gu, S., He, Q., Shen, W., Wang, Z., Wang, D., Hu, Q., Li, Y., Wang, S., Deng, Y., 2022. iNAP: An integrated network analysis pipeline for microbiome studies, Imeta 1, e13. https://doi.org/10.1002/imt2.13.
[47] Seemann, T., 2014. Prokka: rapid prokaryotic genome annotation, Bioinformatics 30, 2068-2069. https://doi.org/10.1093/bioinformatics/btu153.
[48] Lam, T.J., Stamboulian, M., Han, W., Ye, Y., 2020. Model-based and phylogenetically adjusted quantification of metabolic interaction between microbial species, PLoS Comput. Biol. 16, e1007951. https://doi.org/10.1371/journal.pcbi.1007951.
[49] Xu, W.B., Blowes, S.A., Brambilla, V., Chow, C.F.Y., Fontrodona-Eslava, A., Martins, I.S., McGlinn, D., Moyes, F., Sagouis, A., Shimadzu, H., van Klink, R., Magurran, A.E., Gotelli, N.J., McGill, B.J., Dornelas, M., Chase, J.M., 2023. Regional occupancy increases for widespread species but decreases for narrowly distributed species in metacommunity time series, Nat. Commun. 14, 1463. https://doi.org/10.1038/s41467-023-37127-2.
[50] Domeignoz-Horta, L.A., Cappelli, S.L., Shrestha, R., Gerin, S., Lohila, A.K., Heinonsalo, J., Nelson, D.B., Kahmen, A., Duan, P., Sebag, D., Verrecchia, E., Laine, A.-L., 2024. Plant diversity drives positive microbial associations in the rhizosphere enhancing carbon use efficiency in agricultural soils, Nat. Commun. 15, 8065. https://doi.org/10.1038/s41467-024-52449-5.
[51] Li, Y., Schuldt, A., Ebeling, A., Eisenhauer, N., Huang, Y., Albert, G., Albracht, C., Amyntas, A., Bonkowski, M., Bruelheide, H., Bröcher, M., Chesters, D., Chen, J., Chen, Y., Chen, J.-T., Ciobanu, M., Deng, X., Fornoff, F., Gleixner, G., Guo, L., Guo, P.-F., Heintz-Buschart, A., Klein, A.-M., Lange, M., Li, S., Li, Q., Li, Y., Luo, A., Meyer, S.T., von Oheimb, G., Rutten, G., Scholten, T., Solbach,

M.D., Staab, M., Wang, M.-Q., Zhang, N., Zhu, C.-D., Schmid, B., Ma, K., Liu, X., 2024. Plant diversity enhances ecosystem multifunctionality via multitrophic diversity, Nat. Ecol. Evol. 8, 2037-2047. https://doi.org/10.1038/s41559-024-02517-2.
[52] Bock, K.W., 2016. The UDP-glycosyltransferase (UGT) superfamily expressed in humans, insects and plants: Animal-plant arms-race and co-evolution, Biochem. Pharmacol. 99, 11-17. https://doi.org/10.1016/j.bcp.2015.10.001.
[53] Malik, A.A., Martiny, J.B.H., Brodie, E.L., Martiny, A.C., Treseder, K.K., Allison, S.D., 2020. Defining trait-based microbial strategies with consequences for soil carbon cycling under climate change, ISME J. 14, 1-9. https://doi.org/10.1038/s41396-019-0510-0.
[54] Qiao, M., Ying, G.-G., Singer, A.C., Zhu, Y.-G., 2018. Review of antibiotic resistance in China and its environment, Environ. Int. 110, 160-172. https://doi.org/https://doi.org/10.1016/j.envint.2017.10.016.
[55] Wu, J., Wang, J., Li, Z., Guo, S., Li, K., Xu, P., Ok, Y.S., Jones, D.L., Zou, J., 2023. Antibiotics and antibiotic resistance genes in agricultural soils: A systematic analysis, Critical Reviews in Environmental Science and Technology 53, 847-864. https://doi.org/10.1080/10643389.2022.2094693.
[56] Liu, Z.-T., Ma, R.-A., Zhu, D., Konstantinidis, K.T., Zhu, Y.-G., Zhang, S.-Y., 2024. Organic fertilization co-selects genetically linked antibiotic and metal(loid) resistance genes in global soil microbiome, Nat. Commun. 15, 5168. https://doi.org/10.1038/s41467-024-49165-5.
[57] Venkatesan, M., Fruci, M., Verellen, L.A., Skarina, T., Mesa, N., Flick, R., Pham, C., Mahadevan, R., Stogios, P.J., Savchenko, A., 2023. Molecular mechanism of plasmid-borne resistance to sulfonamide antibiotics, Nat Commun 14, 4031. https://doi.org/10.1038/s41467-023-39778-7.
[58] Li, X.-Z., Barré, N., Poole, K., 2000. Influence of the MexA-MexB-OprM multidrug efflux system on expression of the MexC-MexD-OprJ and MexE-MexF-OprN multidrug efflux systems in Pseudomonas aeruginosa, J. Antimicrob. Chemother. 46, 885-893. https://doi.org/10.1093/jac/46.6.885.
[59] Lu, J., Wang, Y., Jin, M., Yuan, Z., Bond, P., Guo, J., 2020. Both silver ions and silver nanoparticles facilitate the horizontal transfer of plasmid-mediated antibiotic resistance genes, Water Res. 169, 115229. https://doi.org/https://doi.org/10.1016/j.watres.2019.115229.
[60] Jechalke, S., Broszat, M., Lang, F., Siebe, C., Smalla, K., Grohmann, E., 2015. Effects of 100 years wastewater irrigation on resistance genes, class 1 integrons and IncP-1 plasmids in Mexican soil, Front. Microbiol. 6, 163. https://doi.org/10.3389/fmicb.2015.00163.
[61] He, X., Abs, E., Allison, S.D., Tao, F., Huang, Y., Manzoni, S., Abramoff, R., Bruni, E., Bowring, S.P.K., Chakrawal, A., Ciais, P., Elsgaard, L., Friedlingstein, P., Georgiou, K., Hugelius, G., Holm, L.B., Li, W., Luo, Y., Marmasse, G., Nunan, N., Qiu, C., Sitch, S., Wang, Y.-P., Goll, D.S., 2024. Emerging multiscale insights on microbial carbon use efficiency in the land carbon cycle, Nat. Commun. 15, 8010. https://doi.org/10.1038/s41467-024-52160-5.
[62] Knight, C.G., Nicolitch, O., Griffiths, R.I., Goodall, T., Jones, B., Weser, C., Langridge, H., Davison, J., Dellavalle, A., Eisenhauer, N., Gongalsky, K.B., Hector, A., Jardine, E., Kardol, P., Maestre, F.T., Schädler, M., Semchenko, M., Stevens, C., Tsiafouli, M.A., Vilhelmsson, O., Wanek, W., de Vries, F.T., 2024. Soil microbiomes show consistent and predictable responses to extreme events, Nature 636, 690-696. https://doi.org/10.1038/s41586-024-08185-3.
[63] Morris, J.J., Lenski, R.E., Zinser, E.R., 2012. The Black Queen Hypothesis: evolution of

dependencies through adaptive gene loss, mBio 3. https://doi.org/10.1128/mBio.00036-12.
[64] Liu, H., Zhang, H., Powell, J., Delgado-Baquerizo, M., Wang, J., Singh, B., 2023. Warmer and drier ecosystems select for smaller bacterial genomes in global soils, Imeta 2, e70. https://doi.org/10.1002/imt2.70.
[65] Zhang, Z., Zhang, L., Zhang, L., Chu, H., Zhou, J., Ju, F., 2024. Diversity and distribution of biosynthetic gene clusters in agricultural soil microbiomes, mSystems 9, e01263-01223. https://doi.org/doi:10.1128/msystems.01263-23.
[66] Booth, S.C., Smith, W.P.J., Foster, K.R., 2023. The evolution of short- and long-range weapons for bacterial competition, Nat. Ecol. Evol. 7, 2080-2091. https://doi.org/10.1038/s41559-023-02234-2.
[67] Liu, Z., Yao, X., Chen, C., Zhao, Y., Dong, C., Sun, L., Zhao, J., Zhang, B., Yu, Z., Cheng, D., Zhu, L., Hu, B., 2025. Growth of microbes in competitive lifestyles promotes increased ARGs in soil microbiota: insights based on genetic traits, Microbiome 13, 8. https://doi.org/10.1186/s40168-024-02005-6.
[68] Morlon, H., 2012. Microbial cooperative warfare, Science 337, 1184-1185. https://doi.org/10.1126/science.1227512.
[69] Wang, Y.F., Liu, Y.J., Fu, Y.M., Xu, J.Y., Zhang, T.L., Cui, H.L., Qiao, M., Rillig, M.C., Zhu, Y.G., Zhu, D., 2024. Microplastic diversity increases the abundance of antibiotic resistance genes in soil, Nat. Commun. 15, 9788. https://doi.org/10.1038/s41467-024-54237-7.
[70] Forster, S.C., Liu, J., Kumar, N., Gulliver, E.L., Gould, J.A., Escobar-Zepeda, A., Mkandawire, T., Pike, L.J., Shao, Y., Stares, M.D., Browne, H.P., Neville, B.A., Lawley, T.D., 2022. Strain-level characterization of broad host range mobile genetic elements transferring antibiotic resistance from the human microbiome, Nat Commun 13, 1445. https://doi.org/10.1038/s41467-022-29096-9.

Figures

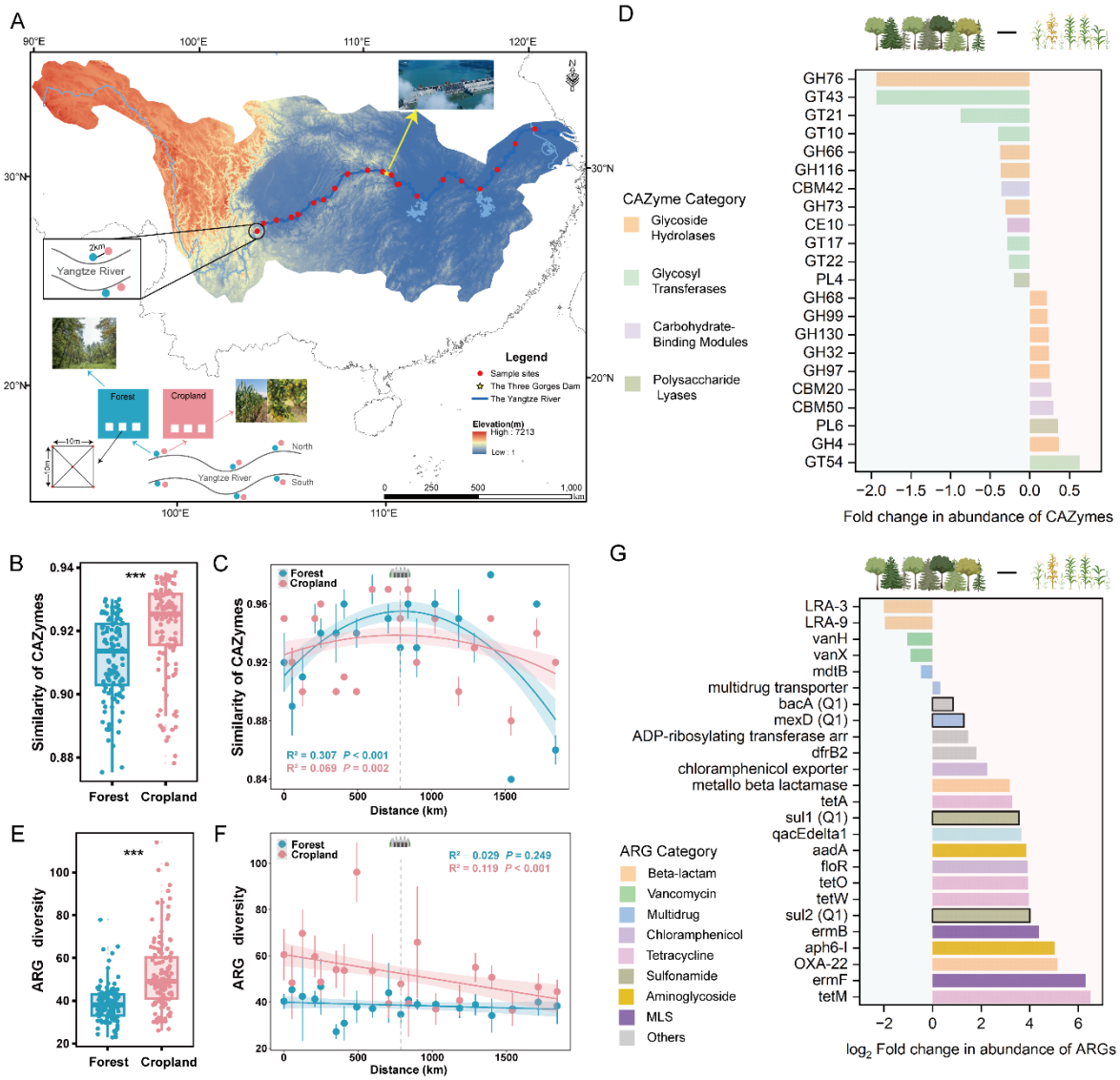


Fig. 1 Microbial functional genes in forest and cropland soils. A Study site location along the upstream-downstream transect of the Yangtze River. **B** CAZyme similarity in forest and cropland soils, with asterisks indicating significant differences (paired t-test, $^{***}p < 0.001$). **C** Correlation between CAZyme similarity and distance from the first sampling site. **D** Fold changes in CAZyme abundance following land-use change, highlighting variables with significant changes ($p < 0.001$). **E** ARG diversity in forest and cropland soils, with asterisks indicating significant differences (paired t-test, $^{***}p < 0.001$). **F** Correlations between ARG diversity and distance from the first sampling site. **G** Log2-fold changes in ARG abundance following land-use change, highlighting variables with significant changes ($p < 0.001$). MLS: macrolide-lincosamide-streptogramin. Distance: cumulative sum of distances between sequential sampling sites, from the first to the last.

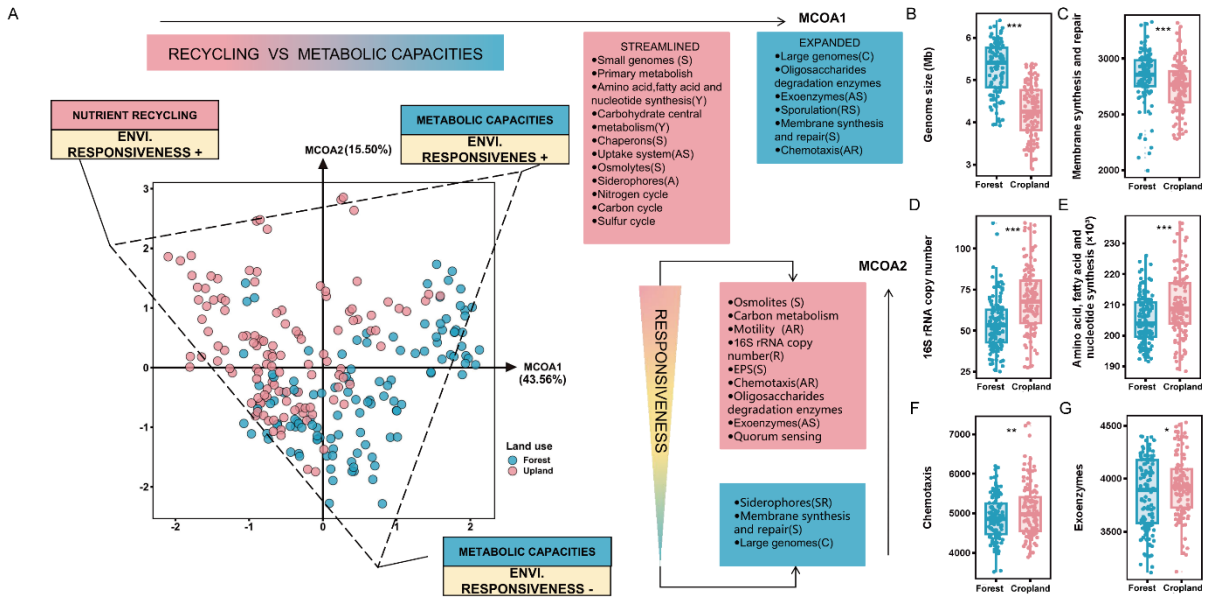


Fig. 2 Microbial life history traits in forest and cropland soils. A Life history strategy of prokaryotic communities in forest and cropland soils. A two-dimensional trait space derived from MCOA illustrates associations between traits across soil prokaryotic communities, with traits inferred from genes enriched in prokaryotic metagenomes. In the trait lists, letters in brackets indicate associations with CSR (competitor, stress-tolerant, ruderal) and YAS (high yield, resource acquisition, stress tolerance) strategies. **B-G** Selected traits (genome size; membrane synthesis and repair; 16S rRNA gene copy number; amino acid, fatty acid and nucleotide synthesis; chemotaxis; exoenzymes) in forest and cropland soils. Asterisks indicate significant differences (paired t-test, $^{***}p < 0.001$, $^{**}p < 0.01$, $^{*}p < 0.05$).

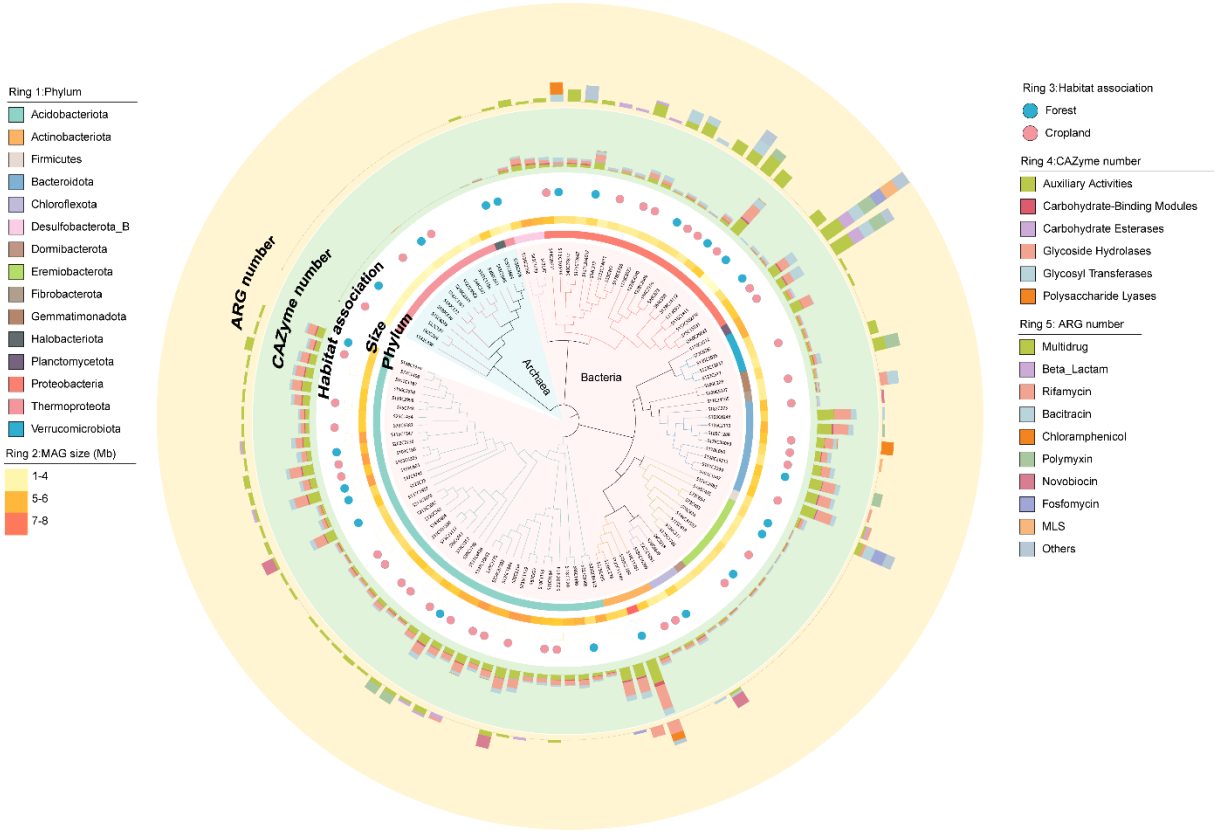


Fig. 3 Metagenome-assembled genomes (MAGs) in forest and cropland soils. High-quality bacterial and archaeal MAGs (> 90% completeness, < 5% contamination) were selected to construct a phylogenetic tree. Branch colors in the first ring (inner to outer) represent individual phyla. The second ring displays MAG size (Mb). In the third ring, blue solid points indicate significantly higher MAG abundance in forest soils, whereas red solid points indicate significantly higher MAG abundance in cropland soils; associations were assigned when this pattern was observed in more than 40% of samples ($p < 0.05$). The fourth ring represents CAZyme diversity across different categories, and the fifth ring shows log2 ARG diversity across categories.

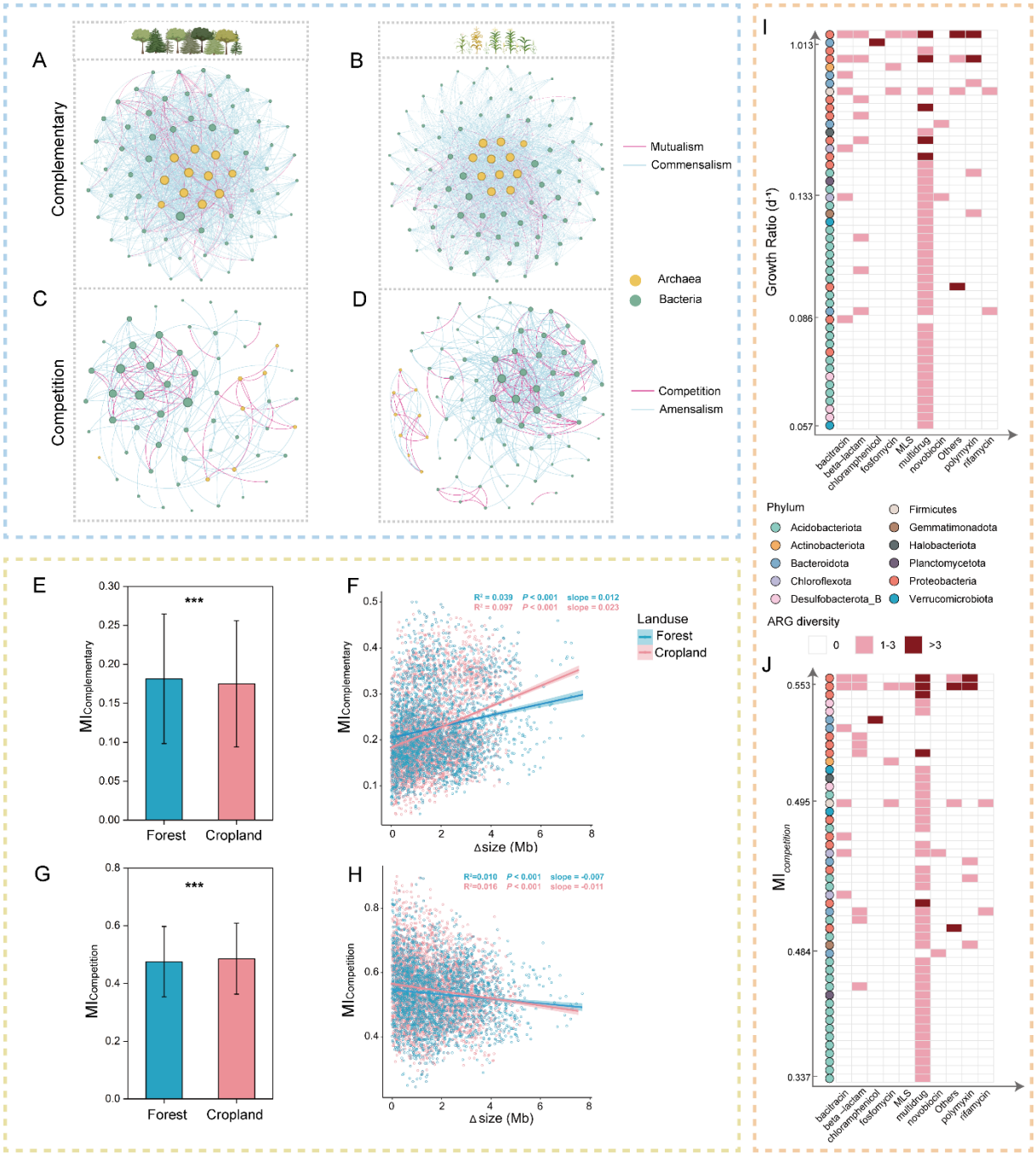


Fig. 4 Microbial metabolic interactions in forest and cropland soils. A,B Distribution of metabolic interactions based on pairwise $MI_{complementarity}$ values in forest and cropland soils. Red links indicate mutualism, while blue links indicate commensalism. **C,D** Distribution of metabolic interactions based on pairwise $MI_{competition}$ values in forest and cropland soils. Red links indicate competition, while blue links indicate amensalism. **E** Pairwise $MI_{complementarity}$ values in forest and cropland soils, with asterisks indicating significant differences (paired t-test, $^{***}p < 0.001$). **F** Correlation between pairwise $MI_{complementarity}$ values and Δsize (pairwise difference in MAG genome size). **G** Pairwise $MI_{competition}$ values in forest and cropland soils, with asterisks indicating significant differences (paired t-test, $^{***}p < 0.001$). **H** Correlation between pairwise $MI_{competition}$ values and Δsize (pairwise difference in MAG genome size). **I** Heatmap of ARG diversity categories across cropland MAGs

ordered by growth ratio. **J** Heatmap of ARG diversity categories across cropland MAGs ordered by $MI_{competition}$. MLS: macrolide-lincosamide-streptogramin.

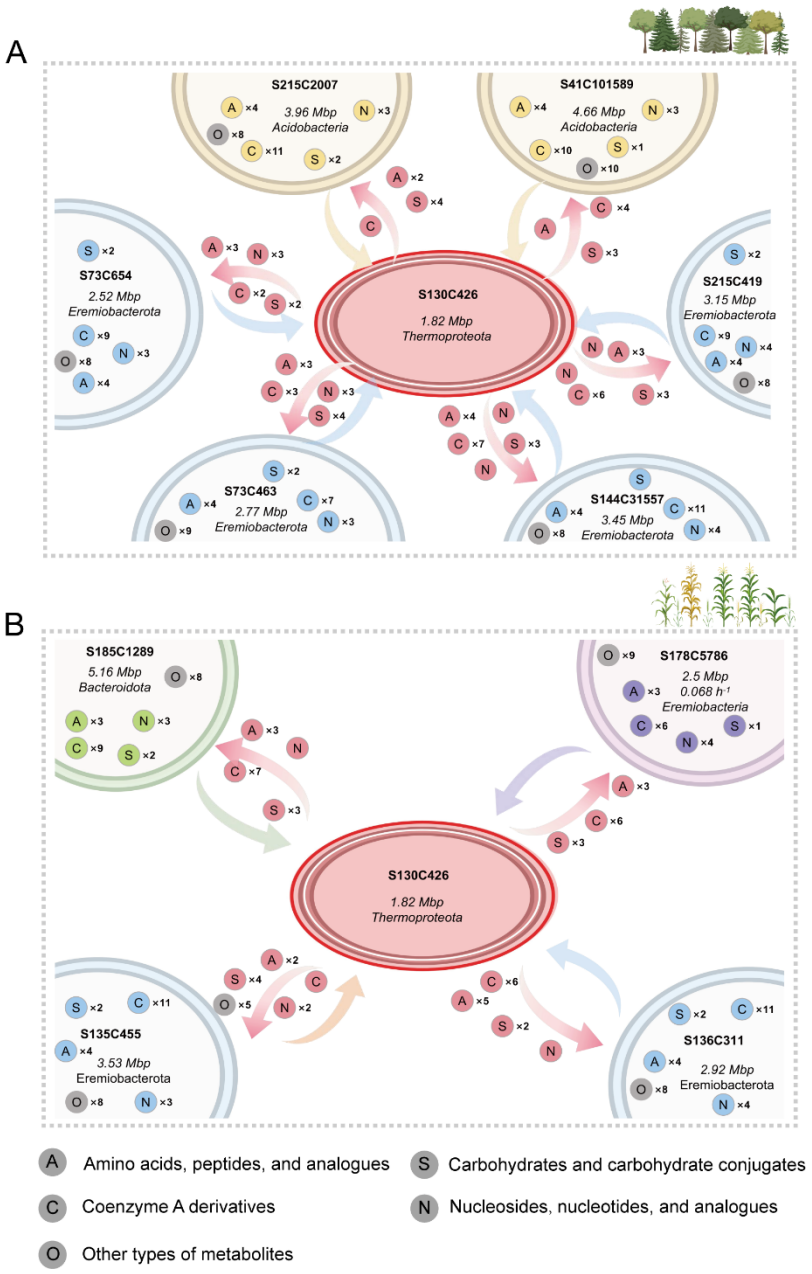


Fig. 5 Potentially transferable metabolite map of forest (A) and cropland (B). The red central oval represents the archaeal MAG *S130C426* (Thermoproteota), while the surrounding-colored ovals indicate bacterial MAGs at the phylum level, with genome sizes labeled inside. Small colored circles represent different metabolites, with numbers indicating their quantities. Arrows denote the direction of metabolite transfer.

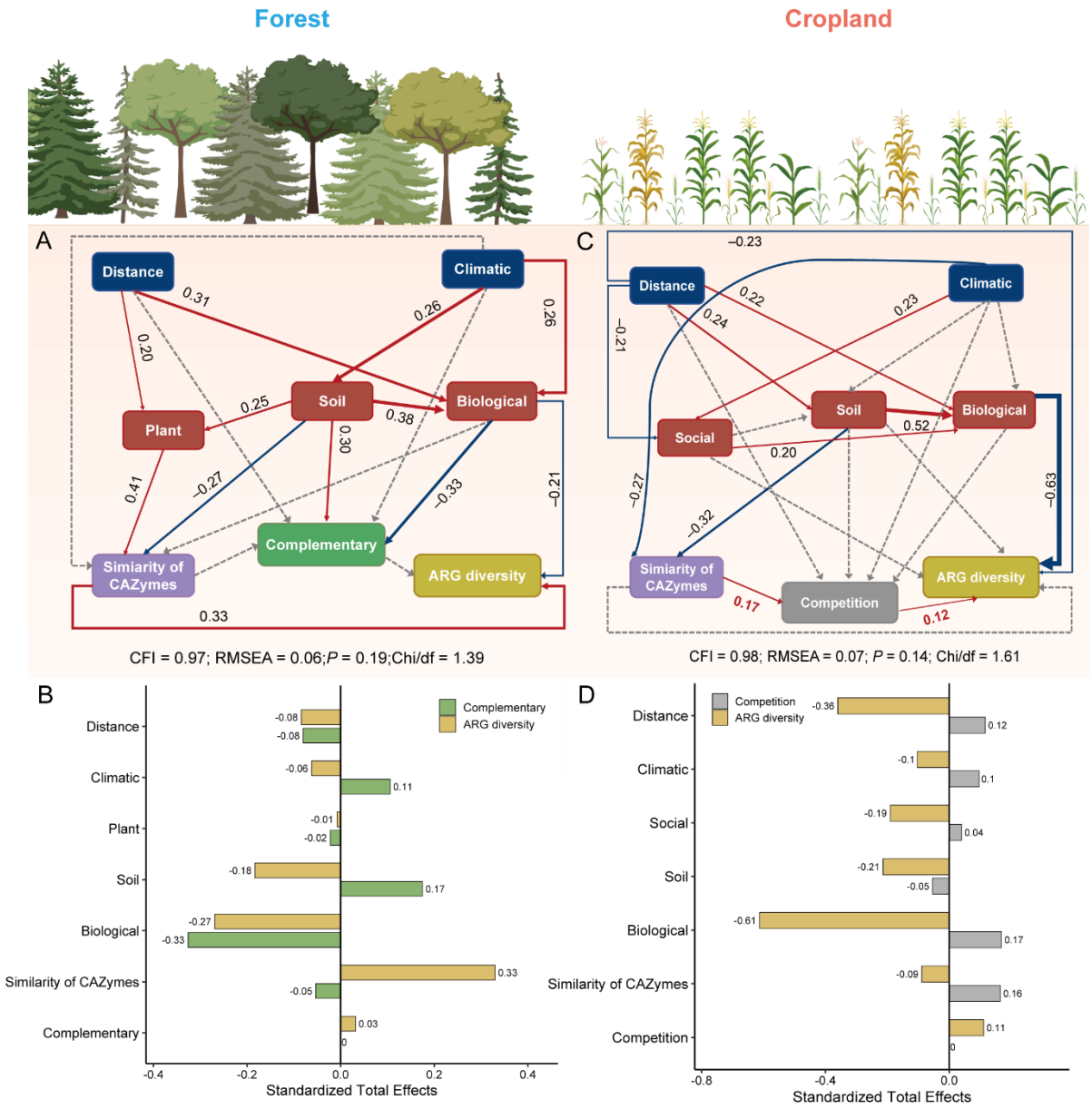


Fig. 6 Driving factors of soil functional homogenization and ARG diversity. A Structural equation model (SEM) depicting relationships among environmental factors, CAZyme similarity, microbial metabolism, and ARG diversity in forest soils. **B** Standardized total effects on microbial complementary and competition, and ARG diversity based on the SEM in panel **A**. **C** SEM depicting relationships among environmental factors, social factors, CAZyme similarity, microbial metabolism and ARG diversity in cropland soils. **D** Standardized total effects on microbial complementary and competition, and ARG diversity based on the SEM in panel **C**. Red and blue arrows indicate significant positive and negative relationships ($p < 0.05$), respectively, while gray dashed lines represent non-significant relationships. Numbers next to arrows denote standardized path coefficients. Distance: Cumulative sum of distances between sampling sites, from the first to the last. Climatic factors: Mean annual temperature and precipitation. Plant factors: Arbor, shrub,

879 and herb richness; litter dry weight. Soil factors: Soil moisture, pH, organic carbon, total nitrogen,
880 total phosphorus, NH_4^+-N, and soil enzymes. Biological factors: Average genome size and 16S
881 rRNA copy number. Social factors: Total population, GDP per capita, agricultural GDP per capita,
882 grain output per unit area, and cropland fertilizer and pesticide use per unit area.

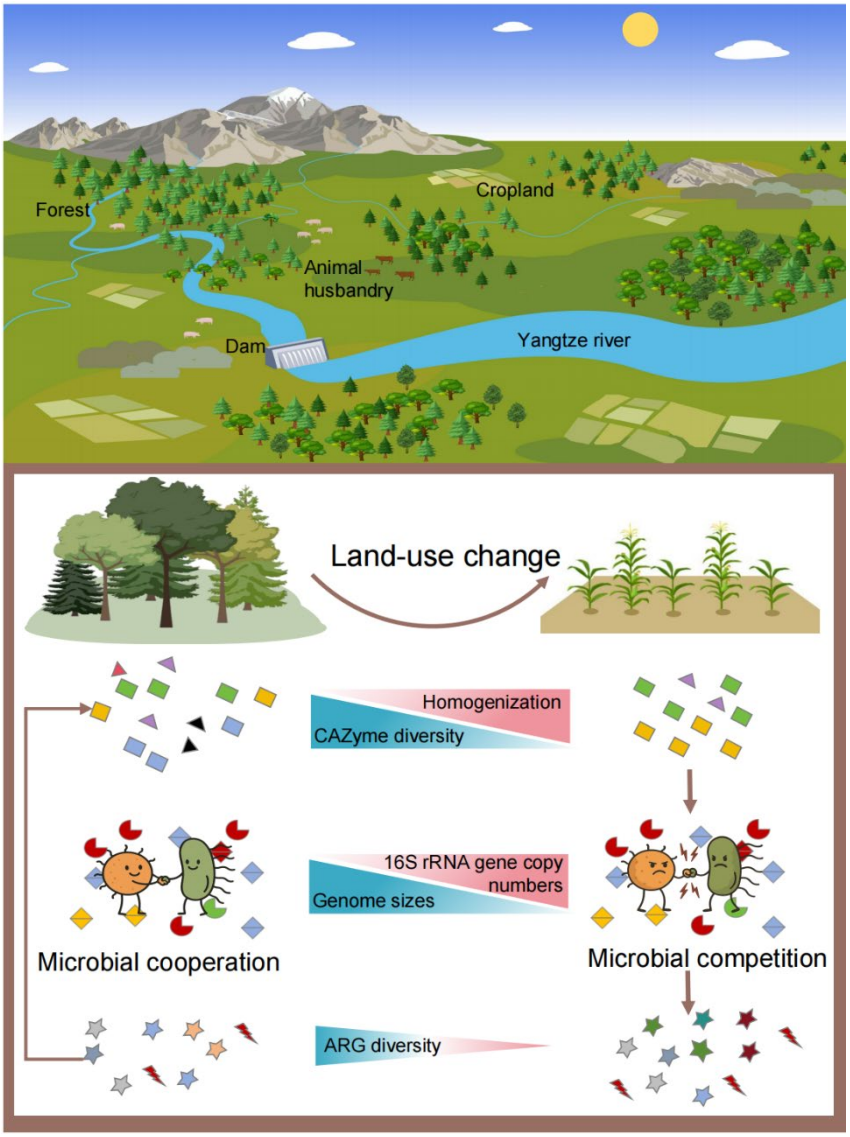


Fig. 7 Conceptual diagrams illustrating the impacts of land-use change on soil microbial homogenization, metabolic relationship, and ARG diversity. The dam is in the middle reaches of the Yangtze River, with cropland and forest ecosystems distributed along its southern and northern banks. The upper reaches have a higher density of aquaculture farms. The bottom left panel represents the forest ecosystem, while the right panel depicts the cropland ecosystem. Arrows indicate increased functional homogenization following land-use change. Blue triangles signify higher indicator values in forests, while red triangles indicate higher values in croplands. Triangles, circles, and squares represent different CAZyme genes, while pentagons and lightning bolts denote ARGs and high-risk ARGs, respectively. The '+' and '-' symbols indicate microbial cooperation and competition.



https://dspace.org/

Carbon metabolic homogenization is linked to microbial competition and antimicrobial resistance in soils under forest-to-cropland conversion

Zhang, Shaoyang; Zhang, Tianlun; Du, Shuai; Yang, Zhugen; Liu, Shengen ...

2026-06-15
Elsevier
https://doi.org/10.1016/j.jhazmat.2026.142281
Zhang S, Zhang T, Du S, et al., (2026) Carbon metabolic homogenization is linked to microbial competition and antimicrobial resistance in soils under forest-to-cropland conversion. Journal of Hazardous Materials, Volume 511, June 2026, Article number 142281

Downloaded from a DSpace repository. https://dspace.org/